energies

MDPI

Review

Research Advances in the Application of the Supercritical CO_2 Brayton Cycle to Reactor Systems: A Review

Yuhui Xiao [1,†], Yuan Zhou [1,†], Yuan Yuan [1,*], Yanping Huang [2] and Gengyuan Tian [1]

[1] College of Physical Science and Technology, Sichuan University, Chengdu 610031, China; 2022222020061@stu.scu.edu.cn (Y.X.); 2021322020027@stu.scu.edu.cn (G.T.)
[2] Nuclear Power Institute of China, Chengdu 610213, China
* Correspondence: yuanyuan21@scu.edu.cn
† These authors contributed equally to this work.

Abstract: Amid the global emphasis on efficient power conversion systems under the "dual carbon" policy framework, the supercritical CO_2 (SCO_2) Brayton cycle is a noteworthy subject, owing to its pronounced efficiency, compact design, economic viability, and remarkable potential to increase the thermal cycle efficiency of nuclear reactors. However, its application across various nuclear reactor loops presents divergent challenges, complicating system design and analytical processes. This paper offers a thorough insight into the latest research on the SCO_2 Brayton cycle, particularly emphasising its integration within directly and indirectly cooled nuclear reactors. The evolution of the Brayton cycle in nuclear reactor systems has been meticulously explored, focusing on its structural dynamics, key components, and inherent pros and cons associated with distinct reactor loops. Based on the theoretical frameworks and empirical findings related to turbomachinery and heat exchangers within the cycle, we chart a course for future enquiries into its critical components, underscoring the indispensable role of experimental investigations. This paper conclusively assesses the feasibility of deploying the SCO_2 Brayton cycle in direct and indirect cooling contexts, offering a forward-looking perspective on its developmental trajectory. The SCO_2 Brayton cycle may become a focal point for research, potentially creating avenues for nuclear energy endeavours.

Keywords: SCO_2 nuclear reactor system; Brayton cycle; direct cooling cycle; indirect cooling cycle

check for updates

Citation: Xiao, Y.; Zhou, Y.; Yuan, Y.; Huang, Y.; Tian, G. Research Advances in the Application of the Supercritical CO_2 Brayton Cycle to Reactor Systems: A Review. *Energies* **2023**, *16*, 7367. https://doi.org/10.3390/en16217367

Academic Editor: Sung Joong Kim

Received: 14 September 2023
Revised: 7 October 2023
Accepted: 16 October 2023
Published: 31 October 2023

Copyright: © 2023 by the authors. Licensee MDPI, Basel, Switzerland. This article is an open access article distributed under the terms and conditions of the Creative Commons Attribution (CC BY) license (https://creativecommons.org/licenses/by/4.0/).

1. Introduction

As the world encounters increasing concerns about the impact of greenhouse gases and the depletion of natural resources, the upcoming 28th Conference of the Parties to the United Nations Framework Convention on Climate Change (COP28) in Dubai in 2023 will be a crucial global event. This convention will explore the intricacies and potential of global climate action [1]. Scientists are currently exploring energy sources that are both economically feasible and environmentally sustainable. Nuclear energy is a promising candidate as it is a low-carbon and secure energy source that can slow resource depletion and ecological degradation [2,3]. Presently, scholars continue to delve deeper into research within the nuclear energy sector. Table 1 provides a succinct introduction to various types of nuclear reactors and their respective characteristics. With ongoing research into nuclear energy in terms of safety and energy conversion efficiency, how to convert nuclear energy into electrical energy safely and effectively has become a focal point in scientists' research in the nuclear energy field [4,5]. Traditional thermodynamic cycles, such as the Rankine cycle and Carnot cycle, typically utilize conventional working fluids like water and air as coolants for the reactor. However, researchers have attempted to enhance the thermal cycle efficiency by replacing the working fluid. Supercritical CO_2 (SCO_2) is a promising option because of its chemical stability, safety, and heat transfer characteristics [6]. SCO_2 is used as the working fluid in the Brayton cycle to convert nuclear energy into electrical power [7].

Table 1. Different reactor types and their used fuels.

Reactor Type	Fuel
Pressurised Water Reactor	Concentrated Uranium Oxide
Boiling Water Reactor	Concentrated Uranium Oxide
Heavy Water Reactor	Natural or Concentrated Uranium Oxide
Gas-Cooled Reactor (coolant is CO_2)	Natural Uranium Metal
High-Temperature Gas-Cooled Reactor	Concentrated Uranium and Thorium Oxide and Carbides
Supercritical Water Reactor	Concentrated Uranium Oxide
Molten Salt Reactor	U, Pu, Th Fluorides
Sodium-Cooled Fast Reactor	Plutonium Oxide and Uranium Oxide
Gas-Cooled Fast Reactor	Depleted Uranium and Any Other Fissile or Breeder Material
Lead-Cooled Fast Reactor	Plutonium, Uranium Metal Alloy

Research on the SCO_2 Brayton cycle began in the 1950s. In 1948, Sulzer Bros secured a patent for a partially condensed CO_2 Brayton cycle, a milestone achieved through the rigorous exploration of SCO_2 [8]. In subsequent decades, particularly the 1960s and 1970s, scientific endeavours in this domain increased [9]. During these years, Feher spearheaded studies focusing on the design and efficiency of the SCO_2 power cycle [10,11]. Building on Feher's foundational work, Angelino et al. investigated supercritical fluids and processes. They explored various cycle layouts to optimise the heat exchanger by reducing the inefficiencies caused by the capacity disparities between the hot and cold sides [6]. Incorporating insights from the Brayton power cycle research, Gokhstein and Dievot assessed the potential of CO_2 as a reactor coolant. They introduced the concept of integrating CO_2 with diverse reactors, which successfully transformed reactor thermal energy into electricity [12,13]. CO_2 was first employed as a reactor coolant in the MAGNOX reactors deployed by the UK and France and was upgraded to Advanced Gas-cooled Reactors (AGRs) in 1970. The valuable experience derived from these operating CO_2-cooled reactors will provide invaluable insights for the design and operation of SCO_2-cooled reactors [14]. Concurrently, studies on turbomachinery, a core component of SCO_2, progressed. However, challenges occurred: the high-density nature of SCO_2 required turbines to withstand intense stress. Furthermore, the wheel disks and blades of the turbines had to be crafted from a single piece, a manufacturing technique that was beyond the capabilities at that time. Additionally, compact heat exchangers and heat sources were limited. Despite the favourable thermodynamic attributes of CO_2 and the potential of the SCO_2 Brayton cycle, harnessing it for nuclear energy applications was significantly challenging, resulting in a slow progress.

In the early 21st century, advancements in printed circuit heat exchanger and CO_2 gas turbine technologies provided new advances for the SCO_2 Brayton cycle. As global concerns over energy and environmental protection intensified, various countries revisited this technology. They recognised its potential to considerably decrease nuclear power costs, ushering in a second wave of research into the SCO_2 Brayton cycle. In 2003, the U.S. Department of Energy initiated an evaluation of SCO_2 [15]. MIT has conducted groundbreaking research into its applications in nuclear reactors. They successfully introduced the concept of a 2400 MW SCO_2 direct-cooled fast reactor, marking the inception of reactors designed with CO_2 as the coolant [8,16–18]. Europe and Japan have also demonstrated significant interest in this area [19,20]. As the relevance of the Brayton cycle in nuclear energy increased, many developing nations participated in the research. The concept of small modular reactors emerged to address the unique challenges encountered by developing countries and isolated off-grid regions—where constructing large-scale civil/commercial nuclear power plants is not feasible [21,22].

By leveraging the adaptability and efficiency of the SCO_2 Brayton cycle, extensive applications have been developed for both direct and indirect reactor cooling cycles. A survey of the recent scholarly literature reveals that much of the current research has

concentrated on its role in indirect cooling, with the exploration of direct cooling still being relatively nascent.

This review discusses the integration of the SCO_2 Brayton cycle within the primary and secondary circuits of reactor systems. It offers a comprehensive overview of the cycle and investigates essential components and reactor design considerations. We aim to present state-of-the-art advancements in the utilisation of SCO_2 in reactor systems, providing readers with insights into the existing challenges and potential future innovations in this domain.

The remainder of this paper is organised as follows: Section 2 introduces the inherent characteristics of the SCO_2 Brayton cycle, detailing its foundational principles, cycle variations, and its respective advantages and disadvantages. Section 3 evaluates the research trajectory of the critical components associated with the cycle, equipping readers with an understanding of the technological evolution. Section 4 outlines the application of the SCO_2 Brayton process in both direct and indirect cooling cycles. In conclusion, we offer a synopsis based on the current research landscape of the SCO_2 Brayton cycle, providing insights into its prospects in reactor system applications.

2. Characteristics of the Supercritical CO_2 Brayton Cycle

2.1. Characterisation of Thermal Properties of Supercritical CO_2

CO_2 has a moderate critical temperature of 304.25 K and a critical pressure of 7.38 MPa, as shown in Figure 1. Its critical point is close to ambient temperature and can be achieved using standard cooling techniques [6]. CO_2 is abundant in nature, exhibits stable chemical characteristics, and is widely used in various industries. When the temperature and pressure surpass its critical points, it enters a supercritical state. Under these conditions, as the temperature increases, SCO_2 consistently remains in a singular phase and its thermophysical properties change continuously. When utilised as a core coolant, it prevents boiling and increases the exit temperature. When employed as a turbomachinery working medium, it prevents gas–liquid separation, thus safeguarding the turbine equipment from potential damage. Additionally, as a heat transfer medium, it prevents phase transitions, eliminates the extended phase-change heat transfer process, and effectively mitigates safety problems [23].

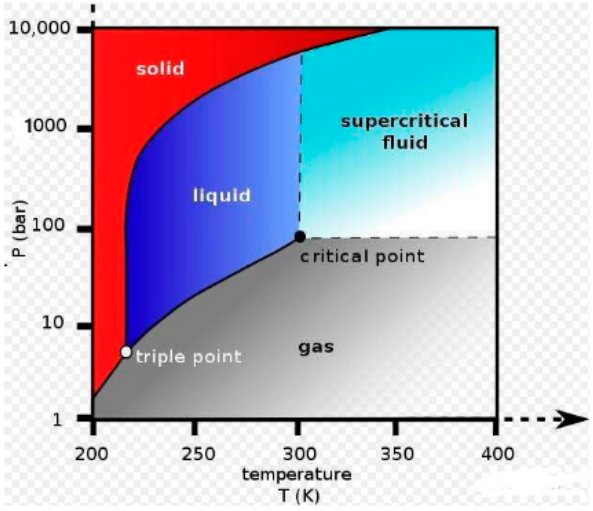


Figure 1. CO_2 three-phase diagram [24].

The phase behaviour of SCO_2 is similar to that of liquids, whereas its viscosity and diffusion characteristics resemble those of gases [25]. SCO_2 exhibits gaseous attributes during expansion but maintains a liquid-like density. However, analysing SCO_2 can be complicated. Figure 2 shows the fluctuation of the constant-pressure specific heat capacity, density, thermal conductivity, and viscosity fluctuation of CO_2 with temperature under

varying pressures. Close to the critical point, the physical properties of CO_2 undergo significant changes. As the pressure approaches this point, the variance in its specific heat ratio becomes even more distinct, with the temperature at the peak specific heat increasing with the pressure. This results in a few challenges: first, the property transitions of SCO_2 near the critical point must be more seamless, causing localised overlaps in flow fields. Second, the parameters at the compressor inlet hover near the two-phase region, possibly resulting in dual zones beneath the critical point [26]. This phenomenon occurs because the blade leading-edge accelerations in the flow field decrease the temperature and pressure of the working mass in certain areas. However, the inherent characteristics of SCO_2 in the proximate critical zone endow it with a remarkable heat-carrying capacity. This significantly influences equipment such as heat exchangers or other devices that employ CO_2 as their working medium. Utilising the high density and amenability to compression of CO_2 enables the compressor inlet temperature to be set close to the critical point, yielding a significant reduction in power usage. The considerable specific heat of CO_2 promotes efficient heat transfer within the exchangers, favouring the design of more compact heat-transfer equipment. Coupled with its low viscosity, this results in diminished flow loss and reduced noise. Consequently, the SCO_2 Brayton cycle is a principal subject of power cycle research [27].

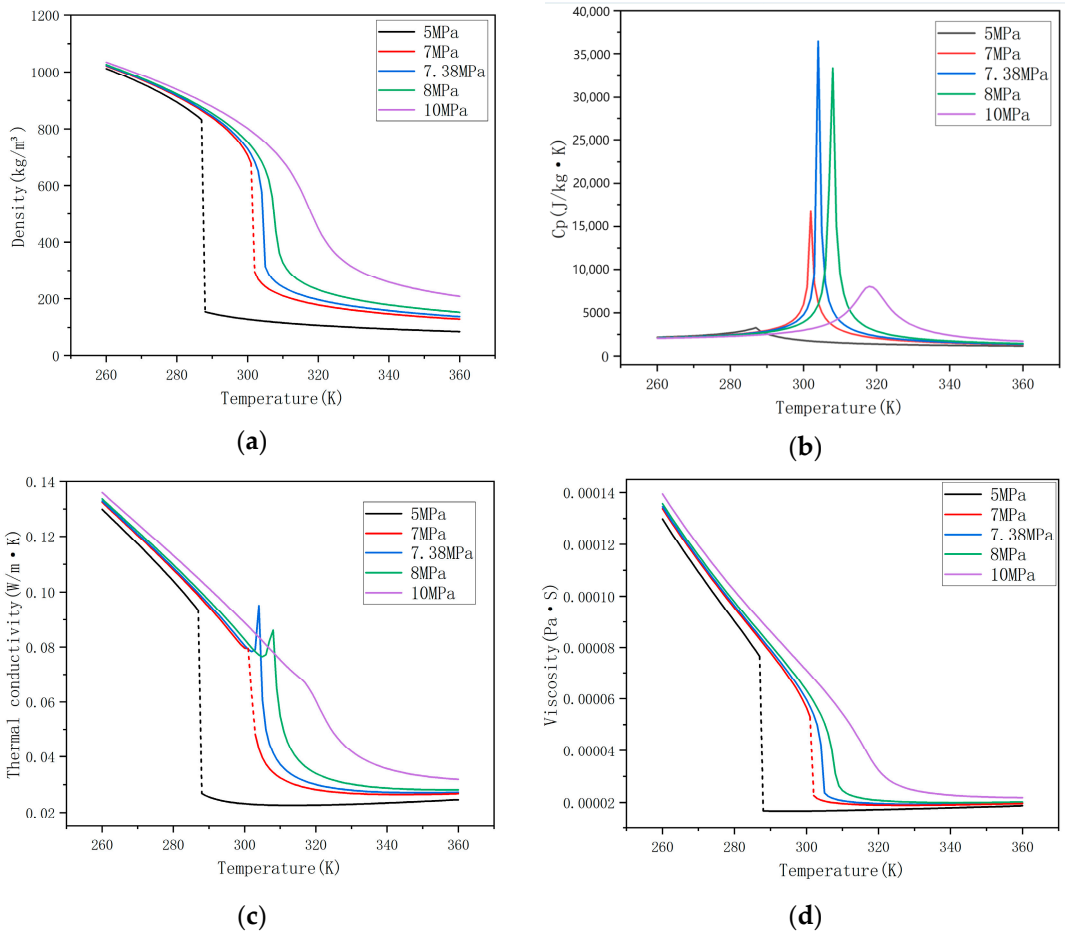


Figure 2. Variation in the thermal properties of CO_2 with temperature at different pressures: (**a**) constant-pressure specific heat capacity, (**b**) densities, (**c**) thermal conductivity, and (**d**) kinematic viscosity. (The critical pressure of CO_2 is 7.38 MPa. When the pressure of CO_2 is below its critical pressure, it undergoes phase changes with increasing temperature, which is represented by dashed lines for subcritical CO_2 phase changes in Figure 2).

2.2. SCO_2 Brayton Cycle

The fundamental Brayton cycle comprises four stages: isentropic compression (1→2, compressor), isobaric heating (2→3, recuperator), isentropic expansion (3→4, turbine), and isobaric cooling (4→1, precooler), as shown in Figure 3. The Brayton cycle system primarily incorporates five components: a heat source, turbine, recuperators, precooler, and compressor. The cycle occurs as follows: (1) The compressor compresses SCO_2, which is subsequently elevated to higher temperatures by the heat source. (2) The heated and pressurised SCO_2, which has high-temperature and high-pressure characteristics, is directed into the turbine machinery. It propels the turbine and drives it to perform mechanical work that powers the generator to produce electricity. (3) After this phase, SCO_2 is channelled into the precooler, which is cooled to its initial temperature and primed for the subsequent cycle.

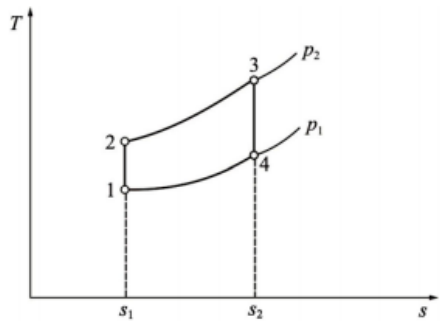


Figure 3. Simple Brayton cycle temperature–entropy diagram.

SCO_2 offers numerous economic and efficiency benefits compared with the Rankine and Brayton cycles when other gases are employed as working fluids. The primary advantages of the supercritical CO_2 cycle are as follows:

(1) Efficiency and performance: The cycle efficiency can exceed 50%, surpassing steam power technologies at medium-to-high temperatures. SCO_2 has a low viscosity and favourable transfer and diffusion characteristics, and its high density facilitates higher fluid pressures with minimal system losses [28]. The absence of a phase change in the circulation process notably diminishes the cycle compression work to only about 30% of the turbine's output power. In contrast, traditional helium cycles utilise compression work, equating to approximately 45% of the turbine's output, whereas gas turbines consume 50–60%. Leveraging multi-stage cycles, a heat source temperature of 550 °C yields a thermoelectric conversion efficiency of approximately 45%. At 700 °C, this efficiency reaches about 50%, surpassing large supercritical steam cycle generators and helium cycle power systems [27].

(2) Compact design: The circulation equipment is compact, miniature, and lightweight. The CO_2 working fluid remains supercritical throughout the cycle, eliminating phase changes and retaining a high density with ample kinetic energy. Compared with steam or helium, turbines require fewer stages and can be designed more compactly. Integrating the turbine and compressor in a coaxial arrangement becomes feasible, resulting in corresponding reductions in the heater, cooler, and auxiliary pipe sizes. The system does not require extensive boiler pipework, resulting in a streamlined compact structure that is conducive to modular assembly. When comparing the turbine volumes required for SCO_2, helium, and steam, the ratio is approximately 1:6:30 [27,29].

(3) Cost savings: SCO_2 is chemically stable and unlikely to chemically react with metals, thus minimising erosion at low-to-medium temperatures. This ensures a high efficiency within these temperature ranges. A broader range of materials can be selected for key system components and circulation parts, simplifying material selection and reducing associated costs.

(4) Operational flexibility: The system design is straightforward, facilitating swift startups, shutdowns, and load tracking, making it particularly suitable for intermittent heat sources [30].

Figure 4 illustrates the relationship graph between thermal cycle efficiency and heat source temperature for different cycles. The pink curve represents the thermal cycle efficiency of the water Rankine cycle; the yellow curve represents the thermal cycle efficiency of the helium Brayton cycle with energy recuperated from one compressor and one turbine; the light blue curve represents the thermal cycle efficiency of the helium Brayton compressor with energy recuperated from three turbines and six compressors, and interstage heating and cooling; and the dark blue curve represents the thermal cycle efficiency of the recompression SCO_2. When the cycle's temperature increases beyond 450 °C, the SCO_2 Brayton cycle has a pronouncedly superior thermal efficiency compared with the Rankine cycle. Additionally, Brayton cycles that use alternate gaseous working media exhibit significantly diminished thermal efficiencies when equipped with only one compressor and turbine, particularly compared with the SCO_2 Brayton cycle. When these Brayton variants incorporate numerous inter-stage heating and cooling phases and operate at temperatures above 700 °C, their efficiencies exceed that of the SCO_2 Brayton cycle. Hence, when evaluating based on cycle power, the SCO_2 Brayton cycle emerges as the prime option in heat source temperatures in the range of 450 to 700 °C.

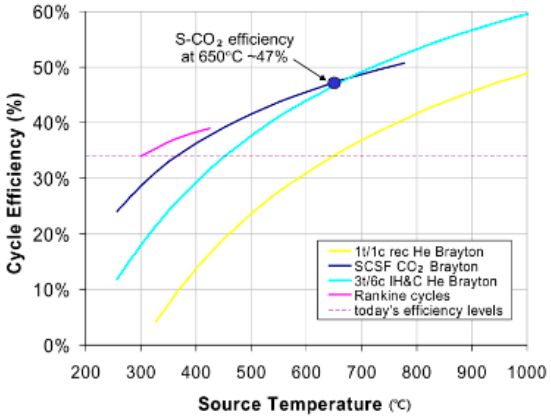


Figure 4. Variation in cycle efficiency with temperature for different gaseous working fluids [25].

Owing to the significant potential of the SCO_2 Brayton cycle, researchers have conducted in-depth studies on its diverse configurations. Figure 5 shows the archetypal design of a conventional SCO_2 Brayton cycle. This design encompasses various iterations, including a simple reheat cycle, recompression cycle, reheating cycle, intermediate cooling cycle, precompression cycle, two iterations of the partial cooling cycle, a dual compression cycle, and an advanced reheat cycle. The detailed cycle parameters for each configuration, complemented by their respective merits and limitations, are listed in Table 2.

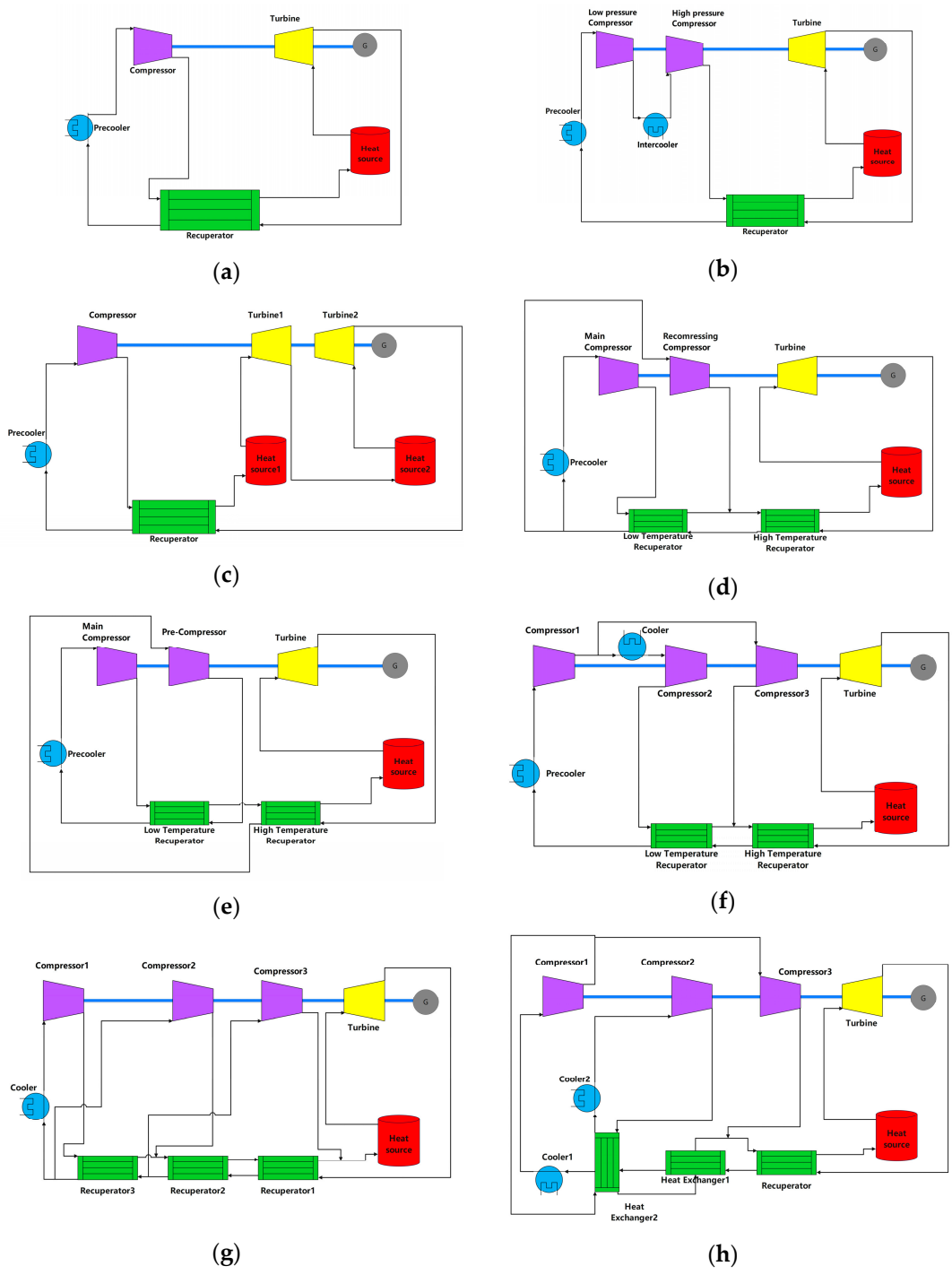


Figure 5. Layout of different Brayton cycles [8,30,31].

Table 2. Characteristics of different types of Brayton cycles [8,30,31].

Number	Cycle Name	P_{min} (MPa)	T_{min} (°C)	P_{max} (MPa)	T_{max} (°C)	Cycle Efficiency	Advantages	Limitations
a	Simple Brayton cycle	7.35	32.0	25.0	550	40.4	The layout is simple; the experimental device is feasible.	A pinch point problem exists, resulting in deterioration of heat transfer. Increased net load.

Table 2. *Cont.*

Number	Cycle Name	P_{min} (MPa)	T_{min} (°C)	P_{max} (MPa)	T_{max} (°C)	Cycle Efficiency	Advantages	Limitations
b	Intercooling Brayton cycle	7.5	32.0	25.0	500	37.0	Simple layout.	Increased net load.
c	Reheating Brayton cycle	7.5	32.0	25.0	500	37.5	Simple layout with significant expansion work	The cycle lacks distinct beneficial features.
d	Recompression Brayton cycle	7.8	32.0	25.0	550	46.5	High thermal efficiency, no 'pinch point' problem, requires less cooling load and can be conducted in a laboratory.	The design of the heat exchanger is relatively complex.
e	Pre-recompression Brayton cycle	9.6	32.0	25.0	550	43.5	No pressure requirement for turbine exhaust.	Complex mechanical design of components.
f	Partial cooling Brayton cycle	5.0	32.0	25.0	550	46.1	High thermal efficiency, large specific work, and low sensitivity to pressure.	Complex layout.
g	Double recompression Brayton cycle	7.5	21.0	20.0	466	39.0	High degree of heat recovery, suitable for sodium-cooled fast reactors.	Complex layout.
h	Modified recompression Brayton cycle	4.4	32.0	15.0	550	45.0	High degree of heat recovery, suitable for sodium-cooled fast reactors.	Complex layout: no significant increase in thermal efficiency compared with re-compression cycles.

Although the SCO_2 Brayton cycle has notable advantages over other contemporary cycles, specific technical challenges remain.

(1) The turbomachinery design has significant complexity. The compressor, which is pivotal to the Brayton cycle, undergoes phase transitions during compression when employing SCO_2. Consequently, this requires intricate considerations of aerodynamic performance, material optimisation, phase transitions, axial loads, operational stability, and sealing mechanisms, particularly when compared with conventional turbomachinery.

(2) Fluid flow and heat transfer mechanisms must be determined. The thermophysical properties of the working fluid, particularly in the context of SCO_2, undergo dramatic shifts near the critical point. Such modifications critically determine heat transfer and flow dynamics, particularly within the microchannels of heat exchangers. The indeterminate nature of these properties across various channels has profound implications for the safety and efficacy of the system and equipment operations.

(3) Research on integrated system characteristics is in its nascent stage. Despite concerted efforts to research the pivotal components of the Brayton system worldwide, a holistic understanding of integrated system functionalities must be revised, thus limiting the subject to experimental methods in the lower-power spectrum [32,33]. Such ambiguities in system dynamics become significantly pronounced when innovative Brayton configurations, such as recompression cycles, are contemplated or when specialised application domains that impose complex operational demands are involved.

3. Advancements in the Study of Key Components in the SCO_2 Brayton Cycle

3.1. Turbomachine

Turbomachinery is a pivotal component of the SCO_2 Brayton cycle and encompasses both turbines and compressors. Through strategic optimisation of this turbomachinery, the

SCO_2 Brayton cycle significantly reduces the compression work, thus enabling a marked decrease in the number of turbine stages required [34].

3.1.1. Turbine

Internationally, numerous universities have embarked on extensive long-term research on SCO_2 turbines. Notably, Sandia National Laboratories in the United States, Tokyo Institute of Technology in Japan, and Korea Institute of Advanced Science and Technology have developed and implemented SCO_2 turbine equipment within their experimental systems, as detailed in Table 3. Other research institutions have focused on the thermodynamic design and aerodynamic analysis of SCO_2 turbines or have engaged in studies to enhance the thermodynamic design models and precision of numerical computation models based on the turbines designed by the institutions mentioned above. However, ongoing challenges exist in the design of turbines for the SCO_2 Brayton cycle. Specifically, designing auxiliary parts such as bearings and seals presents significant difficulties. These SCO_2 turbines often do not achieve their intended operational speeds under experimental settings. For instance, in experiments at the Tokyo Institute of Technology, the combined turbine–compressor unit reached a rotational speed of only 55,000 rpm, which is a notable discrepancy from its design point [35]. Consequently, its efficiency and output power were below the design specifications, highlighting a predominant problem with the current SCO_2 turbine experimental setups.

Table 3. Design parameters of SCO_2 turbines used in experiments [29,31,35,36].

Parameter	SNL	TIT	KAERI
Power/kW	92.0	10.0	82.4
Rotation speed/r·min^{-1}	75,000	100,000	70,000
Flow rate/kg·s^{-1}	3.15	1.2	3.04
Inlet temperature/°C	537	277	180
Inlet pressure/MPa	13.5	11.9	12.98
Impeller diameter/mm	68.30	35.00	48.60
Design efficiency/%	87	75	84

In recent turbine studies, Uusitalo employed computational fluid dynamics (CFD) to investigate the losses associated with SCO_2 centrifugal turbines. Utilising a 1 MW turbine model, he compared the numerical simulation results with melt loss predictions. He observed that consistency between one-dimensional loss coefficients and CFD results can be achieved by adopting a set of appropriate loss correlation coefficients [37]. Another study highlighted that the specific speed and mass flow rate significantly influence the geometric shapes and loss distribution of low-power turbines. The isentropic efficiency of the turbine was optimised at speed ratios ranging from 0.50 to 0.60. When the output power of the centrifugal turbine ranges from 100 kW to several hundred kilowatts, the tip clearance losses are most pronounced. In contrast, the channel, stator blade, and residual speed losses become prominent at higher power levels [38]. Du et al. focused on microturbines with applications of SCO_2 at output powers less than 200 kW, identifying internal and external leakage in the turbines as joint problems [39]. Engeda and Chen delineated and explored classical challenges associated with turbomachinery in the SCO_2 cycle [40]. Cho et al. compared turbine and compressor designs under various operating conditions and independently developed software to validate the experimental data [41]. Lee and Gurgenci contrasted different one-dimensional mean-line design methods, innovative turbines, and advanced partial-load performance prediction models for SCO_2 turbines [42,43]. Unglaube and Chiang employed CFD simulations to compare the performances of several designed turbines to determine the optimal specific speed and speed ratio and observed a positive correlation between turbine expansion and speed ratio [44]. Kumaran et al. refined turbine design algorithms through experimental and numerical studies of a 5 MW SCO_2 Brayton cycle, incorporating actual gas effects for more accurate estimations [45]. Lee

introduced a novel one-dimensional partial-load performance prediction model for SCO_2 centrifugal turbines based on Python. The innovation of the model lies in its precise prediction of partial-load centrifugal turbine performance using fundamental fluid dynamics equations and a natural gas property library, eliminating the need for calibration. Validated through reliable three-dimensional CFD simulations, the results showed a deviation of less than 10% [43]. Son et al. demonstrated the efficacy of neural network algorithms in devising non-design methods for turbine development using a simple Brayton cycle [46].

Compared with international endeavours, research on SCO_2 turbines in China has commenced relatively recently, focusing on the thermodynamic design, aerodynamic analysis, and structural design phases.

Dongbo et al. conducted the thermodynamic and meridional design of a 200 kW SCO_2 centrifugal turbine. They established nozzle and impeller shapes and performed a comprehensive aerodynamic analysis and attained notable efficiency levels [47]. A design introducing partial airflow at the nozzle section was proposed to enhance the inlet blade height of the SCO_2 turbine impeller, making fabrication more straightforward and diminishing secondary flow losses [48]. Hanzhen et al. designed a 15 MW axial-flow SCO_2 turbine and a 1.5 MW centrifugal turbine. An aerodynamic analysis of both turbine types revealed a potential low-pressure area below the critical pressure at the trailing edges of the impeller blades. They also considered the pressure loads and performed a strength check for both impeller types, essentially finalising the design process for the SCO_2 turbine component [49]. Zhang et al. developed in-house codes for the geometric design and performance prediction of an SCO_2 turbine by studying the influences of compression ratio, temperature, and pressure on the cycle [50]. Wang et al. adopted deep-neural network-assisted design techniques [51] and used genetic algorithms to develop a SCO_2 Brayton cycle. Validations using coupled system component models confirmed the reliability of this approach [52]. Zhu studied a bladed SCO_2 centrifugal turbine intake volute and performed numerical simulations of the entire centrifugal turbine [53]. The results indicated a harmonious match between the designed bladed centrifugal turbine intake volute and its nozzle and impeller. Wu created and optimised a SCO_2 centrifugal turbine by performing CFD simulations under design and off-design conditions [54]. The turbine performance was assessed using tip clearance analysis. The results indicated that the turbine output power and total-to-static efficiency were 1.16 MW and 85.36%, respectively. The maximum deviation between the design and simulation results was 3.73%, indicating the reliability of the design model. Numerical simulations ensured that the turbine maintained excellent performance in both design and non-design states. Yang emphasised that the leakage flow in the rear cavity of a centrifugal turbine impeller and the axial forces acting on the impeller play pivotal roles in shaping the aerodynamic performance of a turbine [55].

An integrative review revealed the following insights: thermodynamic design research for SCO_2 centrifugal turbines still requires further exploration to develop methodologies that are more closely aligned with actual operational conditions. Through international and domestic aerodynamic analyses, we observed that the SCO_2 working fluid expands near the critical pressure at the trailing edges of turbine blades. This expansion induces significant changes in the properties of the working fluid, resulting in a transcritical phenomenon in the low-pressure region at the trailing edges, which consequently causes aerodynamic instability. Currently, a challenge lies in structurally optimising turbine blades to mitigate this transcritical effect and enhance their aerodynamic performance, power, and efficiency. Further research is required in this regard. Moreover, during the actual operation of the SCO_2 turbine, the reliability of the bearing and sealing structures is crucial. Refining the design of a turbine and its ancillary components is essential to guaranteeing its aerodynamic performance. Increased research in this area has significant value.

3.1.2. Compressor

Compressors can be categorised into axial and radial types based on the direction of the working fluid flow [56]. Radial compressors, also known as centrifugal compressors,

have attracted increasing interest among researchers owing to their comprehensive operational range, extended axial length, and potential to achieve high efficiency at relatively lower rotational speeds than axial compressors. Compressors are critical for all SCO_2 Brayton cycle systems up to 300 MW, and the power consumed significantly affects the overall system efficiency. Consequently, optimisation of the compressor design and performance analysis is essential [9]. A primary challenge in compressor design results from the significant thermophysical property changes that result in actual gas effects [57]. As a pressurised component within a cycle system, the performance of the compressor directly determines the efficiency of the cycle. Centrifugal compressors have been extensively studied compared with axial compressors owing to their broader operational range and capability to achieve higher pressure ratios (PRs) [58–60].

Park et al. confirmed the superior efficiency of centrifugal compressors [61]. Jeong et al. predicted the off-design performance of SCO_2 compressors and found a direct correlation between the efficiency corrected for density and the accuracy of the projections [62]. Kim et al. proposed an external loss model for SCO_2 compressors by observing that the condensation within the impeller has no significant impact [63]. Building on this, Li et al. considered the system parameters that affect the compressor condensation [64]. Oh et al. compared SCO_2 and air compressors, noting that the sweep angle of the SCO_2 compressor impeller can be modulated through inventory control [65]. Du et al. formulated a one-dimensional design and analysis model for SCO_2 compressors, achieving errors within 10% and computational discrepancies of less than 5% for impeller and expander exits [66]. Xia et al. introduced a 5 MW SCO_2 simple regenerative cycle for small lead-cooled fast reactors. Subsequently, a compressor system design and multidimensional performance optimisation methodology were developed based on this cycle [67]. Through numerical simulation, Pei et al. analysed the causes of blade leading-edge condensation and its impact on compressor performance. They suggested a corrective approach to enhance the flow behaviour at the blade's leading edge, resulting in a 1.411% improvement in the compressor isentropic efficiency and a 0.0353 increase in the pressure ratio [68]. Additionally, they examined the effect of varying the compressor inlet temperatures on the performance under different operating conditions and thermal loads [69].

In reviewing the aforementioned studies, we observe that thermodynamic design research on SCO_2 centrifugal compressors has reached a significant level of sophistication. However, further exploration requires a more accurate thermodynamic design method that closely aligns with real-world operating conditions. The reliability of bearings and sealing structures is paramount during both the experimental research and practical operation of SCO_2 compressors. Refining the design of the compressor and its auxiliary components is essential for ensuring optimal aerodynamic performance. A deeper investigation of this domain is critical.

3.2. Heat Exchanger

Beyond turbomachinery, the heat exchanger is another principal component of the SCO_2 Brayton cycle. By leveraging the unique physical properties of SCO_2, the heat exchanger of the SCO_2 Brayton cycle can be miniaturised, endowing the system with enhanced efficiency and flexibility. However, with the current prominence of recompression cycles [3], the heat exchangers in the SCO_2 Brayton cycles bear significant thermal loads. This can significantly affect the overall system efficiency and its load-following characteristics. Therefore, compact heat exchangers with both a high heat transfer capacity and low pressure drop must be selected for integration into the SCO_2 Brayton cycle. Depending on the type of passageway in the heat exchanger, the designs can be categorised as straight, serrated (or wave-like), S-shaped, or airfoil channels [70,71]. The following Table 4 provides an analysis of the advantages and disadvantages of each channel type.

Table 4. Characteristics of heat exchangers with different channel types.

Type of Channel	Characteristic
Straight channel	The structure is straightforward, has a high degree of technical maturity, and is cost-effective. However, its heat exchange capability is limited. It is suitable for applications requiring a lower pressure drop or systems with unique requirements [72].
Serrated channel	This type of heat exchanger is the most commonly used. Increasing the heat transfer surface area and local flow speed at the channel's bending points significantly enhances its heat transfer capacity [73].
S-shaped channel	Its pressure drop is only a fifth of that of traditional zigzag structures, and the frictional pressure drop is 4–5 times lower than that of serrated designs [74,75].
Airfoil channel	It can reduce pressure drops by half when maintaining equivalent heat exchange performance. The streamlined fin shape effectively suppresses the formation of separation flows [76].

In recent years, the printed circuit heat exchanger (PCHE) designed for SCO_2 Brayton cycles in nuclear reactors has attracted significant interest from researchers worldwide. Li et al. developed an integrated model to analyse the influence of the thermal–hydraulic performance of a heat exchanger on the cycle efficiency and concluded that high Reynolds numbers fail to significantly enhance the cycle efficiency [77]. Liu et al. conducted simulations based on the design conditions of a Brayton cycle power-generation system for ships and derived new thermal relationships for SCO_2 heat exchangers [78]. Liu et al. employed numerical simulations to study the heat transfer characteristics of vertical straight channels in a PCHE under uniform and nonuniform heating conditions [79]. Liu et al. proposed a zigzag-configured PCHE with a honeycomb arrangement to improve fin efficiency and numerically simulated its enhanced thermal performance [73]. Saeed et al. used machine learning algorithms to reduce the overall thermal–hydraulic performance of a C-type PCHE, achieving geometrical structure optimisation improvements of 21% and 16% for the cold and hot sides, respectively [80]. They devised a multilayered approach that merged 3D Reynolds-averaged Navier–Stokes models, artificial neural networks, and internal precooler design and analysis codes to explore various parameters for the precooler design in SCO_2 cycles [81]. Safari et al. introduced triangular and trapezoidal channels as substitutes for conventional circular tubes to enhance the heat transfer capabilities of PCHE. Their findings highlighted that at a Reynolds number of 13,000, the heat transfer efficiency of trapezoidal channels surpassed that of triangular channels by approximately 48%, thereby demonstrating optimal heat transfer performance [82].

Robey et al. used additive manufacturing techniques and piranha pin-fin (PPF) heat exchangers for SCO_2 applications. By adjusting the design parameters and using 3D conjugate heat transfer numerics, they identified an optimal PPF heat exchanger, positioning it as a potential alternative to the PCHE [83].

Additionally, research on heat exchangers for SCO_2 Brayton cycles coupled with various advanced reactors is steadily progressing. Lu et al. optimised a microchannel heat exchanger in a SCO_2 Brayton cycle system for lead-based reactors owing to its low flow resistance and high heat transfer efficiency, rendering it suitable for power conversion systems in lead-based reactors [84]. Riahi et al. simulated 18 distinct channel types and systematically evaluated their heat transfer capabilities using straight channels on the sodium side and various media on the SCO_2 side [85]. Su et al. compared contemporary models and numerical methodologies with the experimental data of lead–bismuth eutectic (LBE) cooling tubes and simulation data of conjugate heat transfer in straight PCHE channels between LBE and SCO_2. They recreated the flow and heat transfer processes of SCO_2 in PCHE linear channels and examined the conjugate heat transfer characteristics between the LBE and SCO_2 in these channels [86].

The PCHE is efficient and compact, making it a logical option for SCO_2 Brayton cycle applications. However, experimental and theoretical analyses in this domain are limited. More comprehensive investigations into the fundamental thermal–hydraulic characteristics of SCO_2 within the PCHE are urgently required. These methods include advanced experimental measurement techniques and precise numerical simulations. Considering factors such as heat transfer, pressure resistance, maturity, and manufacturing costs, zigzag-shaped channels have emerged as the preferred channel type for SCO_2. Optimising the geometric and operational parameters should minimise the pressure drop in zigzag-channel PCHEs. Despite extensive research on flow characteristics and heat transfer performance, the current stage reveals several areas for improvement. These gaps provide a roadmap for an in-depth PCHE research:

(1) Compared with traditional shell-and-tube heat exchangers, more mature empirical formulas are required for heat exchanger design. Some studies have indicated that the equations derived from numerical simulations and experimental research align well under laminar flow conditions. However, discrepancies remain under turbulent conditions.
(2) Although numerous researchers have suggested that the heat transfer performance of S-shaped and wing-shaped channel PCHEs is superior to that of zigzag and flat straight shapes, the current manufacturing complexities of S-shaped and wing-shaped channels indicate that, from a cost-economic perspective, zigzag or flat straight PCHEs might still be the optimal options. Therefore, cost-effective manufacturing techniques must be developed for intricate-channel PCHEs.

4. Progress of SCO_2 Brayton Cycle Research in the Field of Reactors

4.1. Application of the SCO_2 Brayton Cycle to Direct-Cooled Reactors

The use of the SCO_2 Brayton cycle in reactors varies depending on its placement in the primary or secondary loop of the reactor. When integrated into the primary loop, the SCO_2 Brayton cycle merges the reactor with the coolant circulation, eliminating the intermediary heat exchanger. This consolidation reduces the volume and achieves a more compact reactor design. However, integrating the SCO_2 Brayton cycle into the reactor's primary loop introduces challenges to the circuit and core design of the system. As a result, primary loop designs primarily favour simple or recompression Brayton cycles. Table 5 provides detailed information on various reactors and their specific parameters.

Table 5. Brayton cycle used for the primary loop of the reactor and reactor research.

Organisation	Cycle Layout	Parameters	Value	Reactor Studies
MIT	Recompression Brayton cycle	Thermal power/MW	2400	A 2400 MW Brayton re-compression cycle was designed, with reactor efficiency surpassing 50%, achieving a 2% improvement over conventional cycles. This implementation comprises four circuits, each with a capacity of 600 MW [16,18].
		Coolant type	SCO_2	
		Fuel type	UO_2/BeO	
		Coolant pressure/MPa	20	
		Reactor inlet temperature/°C	485.5	
		Reactor outlet temperature/°C	650	
		Reactor power density/(kW/L)	85	
		Fuel power density/(kW/L)	151	
		Thermal efficiency/10^{-2}	50.8	
		Axial power shape	Chopped cosine	
		Coolant fraction/10^{-2}	25	

Table 5. *Cont.*

Organisation	Cycle Layout	Parameters	Value	Reactor Studies
Sandia National Laboratories	Recompression Brayton cycle	Reactor thermal power/MW	200	The primary advantages of the SCO_2-GFR include a high thermal efficiency of 45% to 50% even at a relatively low reactor outlet temperature (650 °C); a compact and cost-effective power conversion system; the potential for a long-life core and closed fuel cycle; and ensuring a minor reactivity due to coolant loss, and a natural convection-led decay heat removal [25].
		Fuel type	UO_2/MOX	
		Cycle thermal efficiency/10^{-2}	50	
		Output power/MW	100	
		Reactor pressure/MPa	20.0	
		Compressor inlet pressure/MPa	7.0	
		Reactor inlet temperature/°C	450	
		Reactor outlet temperature/°C	650	
		Reactor mass flow rate (kg/s)	920	
		Reactor power density (kW/L)	55.1	
		Core pressure drop/MPa	<0.3 MPa	
		Reactor life/a	20	
		Average fuel burnup/(MW/d·t)	71,000	
		Specific power (kW/kg)	10.0	
KAIST	Simple Brayton cycle	Reactor thermal power/MW	36	The Brayton simple cycle was adopted to reduce the occupied volume of the heat exchanger, drum-shaped control rods were employed to minimize axial volume, and a double-walled safety shell was incorporated [87–89].
		Fuel type	UN	
		Coolant pressure/MPa	20	
		Coolant velocity/(m/s)	6.92	
		Coolant inlet temperature/K	655	
		Coolant outlet temperature/K	823	
		Coolant volume fraction/10^{-2}	30.6	
		Fuel volume fraction/10^{-2}	54.5	
		Component volume fraction/10^{-2}	14.9	
Xi'an Jiaotong University	Simple Brayton cycle	Core thermal power/MW	300	The system is characterised by innovative fast gas reactor technology and advanced structural and cladding materials, resulting in excellent economic and safety features. The primary assembly parameters were selected to maximize fuel spacing with minimal excess reactivity, minimising material temperature and coolant void reactivity [90].
		Fuel type	UO_2	
		Core outlet temperature/°C	500	
		Core pressure/MPa	14	
		Mass flow rate/kg/s	1254	
		Power density/MW/m^3	36.5	
		Cycle length/year	20	
		Thermal efficiency/	40%	
		Mass flow rate (kg/s)	26.3	
		Turbine isentropic efficiency	79%	
		Compressor isentropic efficiency	78%	
		System efficiency	22.4%	
		Net power output/MW	1.12	
North China Electric Power University	Simple Brayton cycle	Reactor power/kW	3.30	A conceptual design for a SCO_2 direct-cooled 1 MWe offshore floating nuclear power station (SCFNP-1) was proposed. Considering the lower flow rates of small-power systems, a pre-pressurised safety shell was incorporated to ensure system safety under LOCA conditions [91,92].
		Fuel type	$U^{15}N$	
		Net power/MW	1.00	
		Inlet temperature of turbine/°C	550.00	
		Outlet temperature of turbine/°C	442.60	
		Inlet temperature of compressor/°C	60.00	
		Outlet temperature of compressor/°C	142.10	
		Inlet pressure of turbine/MPa	19.60	
		Outlet pressure of turbine/MPa	8.02	
		Inlet pressure of compressor/MPa	8.01	
		Outlet pressure of compressor/MPa	20.04	
		Mass flow rate of main loop/kg/s	15.10	
		Inlet temperature of cooling source/°C	45.00	

Table 5. *Cont.*

Organisation	Cycle Layout	Parameters	Value	Reactor Studies
		Outlet temperature of cooling source/°C	131.09	
		Mass flow rate of cooling source/kg/s	13.67	
Xi'an Jiaotong University	Simple Brayton cycle	Total power/kWe	100	Thermo-hydraulic design and mass optimisation studies were conducted for a 100 kW reactor system intended for Martian surface deployment. Because radiators significantly contribute to the system's mass, future radiator mass models require an upgrade. Additionally, integrating intelligent optimisation algorithms is imperative for assessing the impact of various parameters on the system [93].
		Fuel type	UO_2	
		Compressor inlet pressure/MPa	9	
		Compressor outlet pressure/MPa	18	
		Compressor inlet temperature/K	433	
		Turbine inlet temperature/K	900	
		Compressor efficiency	0.8538	
		Recuperator conductance/kW·K^{-1}	35.92	
		Heat sink temperature/K	200	
		Radiator approach ΔT/K	10	
		Coolant	CO_2	

Although direct SCO_2 cooling of reactors can make the entire cycle more compact and effectively reduce costs, new designs and evaluations of SCO_2-cooled reactors are still required. This requirement implies that the research efficiency and timelines encounter significant delays.

4.2. Application of the SCO_2 Brayton Cycle to Indirectly Cooled Reactors

When the SCO_2 Brayton cycle is implemented in the secondary loop system of a reactor, SCO_2 serves as the intermediate working fluid, absorbing heat at high temperatures and pressures. This heat is then transitioned into mechanical energy via the turbomachinery, ultimately generating electrical energy. Researchers can bypass the initial conceptual reactor design by focusing on the indirect energy cycle with SCO_2 and directing their attention to the design and optimisation of the cycle. This method streamlines the research and design phases of SCO_2 nuclear power systems, ensuring that new reactors achieve compact system volume and high thermal efficiency in their cycles.

Recent research worldwide has shown that various nuclear reactor types can utilise the SCO_2 Brayton cycle. These include high-temperature gas-cooled, sodium-cooled fast, and lead-cooled fast reactors. Table 6 provides the details of the specific applications.

Table 6. Brayton cycle used for the reactor's secondary loop and reactor research.

Brayton Cycle Coupled Core Type	Author	Cycle Layout	Technical Characteristics
Pressurised water reactor	Fana et al. [94]	Recompression Brayton cycle	By integrating the SCO_2 recompression Brayton cycle with the transcritical CO_2 cycle, we can achieve a peak cycle efficiency of 65.7%.
	Hofer et al. [95]	Simple Brayton cycle	We ran simulations on the SCO_2 waste heat discharge systems under various environmental and steam-side boundary conditions.
	Lim et al. [96,97]	Intercooling Brayton cycle + Reheating Brayton cycle + Recompression Brayton cycle	An intermediate cooling cycle has minimal impact on overall cycle efficiency. However, the efficiency gap between cycles with and without a reheating loop reaches up to 4.5%.
	Lee et al. [98]	Recuperated Brayton cycle	Under APR-1400 conditions, the SCO_2 Brayton cycle outperforms the steam power cycle in thermal efficiency.

Table 6. *Cont.*

Brayton Cycle Coupled Core Type	Author	Cycle Layout	Technical Characteristics
Lead-cooled fast reactor	Moisseytsev et al. [99]	Recompression Brayton cycle	The STAR-LM lead-cooled fast reactor concept uses the inherent characteristics of lead coolant, nitride fuel, and reactor system pool configuration to enhance passive safety performance.
	M-J Li et al. [100,101]	Recompression Brayton cycle	The recompressed SCO_2 Brayton cycle LFR power generation system has a cycle thermal efficiency of 43.72%. Compared with traditional steam Rankine and He Brayton cycles, the recompressed SCO_2 Brayton cycle LFR system offers an efficiency of over 40%.
	Wu et al. [102]	Simple Brayton cycle/Recompression Brayton cycle	They developed a lead-fast reactor concept with a core exit temperature of 480 °C. Sensitivity analyses yielded feasible simple and recompressed Brayton cycle designs for this reactor concept under water- and dry-cooling conditions. Water cooling offers optimal cycle efficiencies of 35.9%, whereas dry cooling achieves 32.6%.
	H. Li et al. [103]	Simple Brayton cycle	They conducted comprehensive studies on the design and off-design performance of the SCO_2 power system for small lead-cooled fast reactors. They established off-design condition models for the turbine, compressor, and heat exchanger. The study examined five off-design control strategies under various grid load conditions, linking them to clean production and sustainable development; the system's thermal efficiency peaked at 32.18%.
	Du et al. [104–108]	Recompression Brayton cycle	They created a thermodynamic model for the 10 MW SCO_2-RC and assessed its dynamic characteristics under different conditions. With a bypass ratio of 0.37, the system achieves its highest efficiency of 42.12% and offers the lowest cost per production unit.
Sodium-cooled fast reactor	Moisseytsev et al. [109]	Recompression Brayton cycle	Using the 250 MWt ABTR concept power converter from Argonne National Laboratory, they explored several alternative layouts for the SCO_2 Brayton cycle power conversion for sodium-cooled fast reactors. Adjusting the minimum temperature or pressure can boost the efficiency of the reference recompression cycle by 1%.
	Eoh et al. [110]	Recompression Brayton cycle	They conducted surface reaction tests for the sodium-cooled fast reactor's SCO_2 Brayton cycle at sodium temperatures between 200 and 600 °C and proposed a two-zone reaction model with a threshold temperature of 460 °C. The tests determined the kinetics parameters, such as the activation energy for the reaction zone, and set the model parameters accordingly. Test results show potential sodium-CO_2 interaction behaviour heavily depends on the CO_2 leak location.
	Sienicki et al. [111]	Recompression Brayton cycle	Optimising components and cycle conditions enabled them to cut electricity costs per unit and reduce space requirements for turbine generators and reactor buildings. These results further support the benefits of the SCO_2 Brayton cycle power conversion for SFR.
	Du et al. [60]	Recompression Brayton cycle	They established a thermodynamic model of the sodium-cooled fast reactor's SCO_2 recompression cycle, highlighting the widespread use of two-stage expansion with reheating for improved cycle performance.
	Xie et al. [112]	Recompression Brayton cycle	They analysed system performance and conducted an economic evaluation of the sodium fast reactor's SCO_2 Brayton cycle with a partial cooling layout. They introduced energy, exergy, and energy-economic analyses and compared optimisation results with the recompression cycle.
	Zhang et al. [113]	Simple Brayton cycle	Further optimisation using a genetic algorithm identified optimal conditions: compressor inlet temperature of 304 K, turbine inlet temperature of 912 K, a temperature ratio of 3.0, and a pressure ratio of 3.0. This approach achieved an optimised system efficiency of 0.4057, nearly 30% higher than the earlier efficiency of 0.3123.
High-temperature gas-cooled reactor	Nurmayady et al. [114]	Recompression Brayton cycle	A comparison of helium and CO_2 in the second cycle of the tertiary Brayton cycle showed that CO_2 can reach an efficiency of 52%.

Table 6. *Cont.*

Brayton Cycle Coupled Core Type	Author	Cycle Layout	Technical Characteristics
Molten salt reactor	Yun et al. [115]	Reheating and intercooling Brayton cycle	They designed and optimised the SCO_2 Brayton cycle parameters for thermal efficiency and applied them to the fluoride salt-cooled high-temperature advanced reactor (FuSTAR). Using the particle swarm optimisation (PSO) algorithm, they determined the optimised thermal efficiency for the simple regeneration cycle. Analysing the entropy and temperature differences between cold and hot sources, they proposed four enhanced configurations. Under FuSTAR's thermodynamic boundaries, reheated and intercooling cycles achieve the highest thermal efficiency of 51.64% and serve as the best energy conversion systems for FuSTAR.
Heat pipe reactor	Simao, G et al. [116]	Simple Brayton cycle	Based on the novel 'heat pipe reactor + SCO_2 cycle' nuclear power device concept, rigorous research and design work were conducted, particularly in applications such as oceanic heat pipe reactors, SCO_2 thermodynamic cycles, safety analyses, and intelligent autonomous control methods. Existing research results have created a robust foundation for further refinement and addressing critical technological challenges in novel nuclear power device schemes

Although the SCO_2 Brayton cycle has distinct advantages when applied to both the primary and secondary loops of reactors, shared technical problems and challenges exist across both applications. The corrosion resistance, thermal stability, and mechanical strength of materials must be evaluated under the high-temperature and high-pressure conditions inherent to the SCO_2 Brayton cycle. Moreover, the control strategies and parameter optimisation for the SCO_2 Brayton cycle require more profound investigative research. Furthermore, when compared with the traditional steam Rankine cycles, the SCO_2 Brayton cycle requires the establishment of more comprehensive safety control measures and emergency response systems to address unforeseen incidents and accidents during reactor operation.

The SCO_2 Brayton cycle application is more comprehensive than reactor loops. It extends to other domains, including the chemical engineering, aerospace, solar energy, and automotive industries [23,117–120]. Thus, as an emerging energy conversion technology, the SCO_2 Brayton cycle has significant potential and offers expansive application opportunities.

5. Summary

The SCO_2 Brayton cycle, characterised by its compactness, efficiency, and economic appeal, has broadened research directions in the nuclear energy sector. The layout and critical components of the Brayton cycle profoundly influence the thermal efficiency of a reactor system. Consequently, depending on the differentiation between the primary and secondary loops within the reactor, alterations may occur in the pressure and temperature settings of the Brayton cycle. This paper comprehensively reviews the application of the SCO_2 Brayton cycle in reactor systems, encompassing various layouts in both the primary and secondary loops, advancements in fundamental component research, and empirical studies on these critical parts. This paper offers a succinct retrospective of previous studies and outlines potential directions for further research.

A summary is provided as follows:

(1) Extensively studying the turbomachinery and heat exchangers can enhance our understanding of the transient performance of the SCO_2 Brayton cycle. Our findings reveal that compressors operating near the critical point require more interest to ensure stable and efficient performance under fluctuating loads.

(2) The current optimal options for heat exchangers remain serrated or planar PCHEs owing to their economic viability and technological maturity.

(3) The dynamic characteristics of the SCO_2 Brayton cycle coupled with reactor systems differ significantly from those coupled with other energy types. The dynamic response of the reactor core in the SCO_2 nuclear system is unique and closely intertwined with the dynamic performance of the SCO_2 Brayton cycle, particularly in systems with

direct SCO_2 cooling. An analysis of the existing body of research suggests that applications of Brayton cycle coupling with various reactor types outnumber those focusing only on SCO_2 direct fast reactors. The reasons for this are summarised as follows:

(a) Studies and applications of the SCO_2 Brayton cycle remain relatively nascent. Within the reactor domain, research typically commences with fuel assembly and operational stability before branching to other technologies.
(b) The primary loop in reactors plays a critical role in nuclear fuel cooling and heat transfer, making it an integral part of reactor systems. In contrast, the secondary loop often isolates itself from the primary loop through a working fluid, generating gases that drive the turbomachinery for electricity production. Owing to the direct contact of the primary loop with the nuclear fuel and high-temperature and high-pressure working fluids, the design, operation, and safety protocols are inherently more stringent and intricate.
(c) SCO_2 has distinct physicochemical properties when juxtaposed with conventional working fluids, thus requiring exhaustive experimental and simulation-based evaluations to assess the feasibility and efficacy of the SCO_2 Brayton cycle in primary-loop applications.

Thus, future work can be developed from the following points:

(1) Refining turbomachinery and its auxiliary components is paramount to guaranteeing optimal aerodynamic performance.
(2) Low-cost complex flow-path heat exchangers owing to advancements in additive manufacturing require urgent exploration.
(3) The literature on control strategies remains sparse, making it a burgeoning focal point for future SCO_2 nuclear application studies. Previous studies on reactor systems and control strategies for other SCO_2 Brayton cycle applications offer valuable insights into the formulation of control strategies in a nuclear context.

In conclusion, the SCO_2 Brayton cycle has significant application potential as an energy conversion system. Its feasibility as a direct cooling cycle for nuclear energy, or as an indirect cooling loop in fourth-generation reactor concepts, has been validated by many theoretical and empirical studies. Therefore, advancing research on the application of the SCO_2 Brayton cycle in reactor systems addresses urgent problems in pivotal domains and plays a pivotal role in propelling the development of SCO_2 Brayton reactors.

Author Contributions: Conceptualization, Y.Y., Y.X. and Y.Z.; formal analysis, Y.X.; investigation, Y.X.; resources, Y.X.; data curation, G.T. and Y.H.; writing—original draft preparation, Y.X.; writing—review and editing, Y.X.; supervision, Y.Y. and Y.Z.; project administration, Y.Y. All authors have read and agreed to the published version of the manuscript.

Funding: This research was funded by National Natural Science Foundation of China [12105192], GuangDong Basic and Applied Basic Research Foundation [2020A1515110512] and Funded project by the Key Laboratory of Nuclear Reactor System Design Technology, Nuclear Power Institute of China [HT-KFKT-02-2020002].

Data Availability Statement: Not applicable.

Conflicts of Interest: The authors declare no conflict of interest.

References

1. Twenty-eighth United Nations Climate Change Conference. Available online: https://www.un.org/zh/summits2023 (accessed on 13 September 2023).
2. Gungor, G.; Sari, R. Nuclear power and climate policy integration in developed and developing countries. *Renew. Sustain. Energy Rev.* **2022**, *169*, 112839. [CrossRef]
3. Liu, G.; Huang, Y.; Wang, J.; Liu, R. A review on the thermal-hydraulic performance and optimization of printed circuit heat exchangers for supercritical CO_2 in advanced nuclear power systems. *Renew. Sustain. Energy Rev.* **2020**, *133*, 110290. [CrossRef]

4. Zubair, M.; Ababneh, A.; Ishag, A. Station black out concurrent with PORV failure using a Generic Pressurized Water Reactor simulator. *Ann. Nucl. Energy* **2017**, *110*, 1081–1090. [CrossRef]
5. Zubair, M.; Ishag, A. Sensitivity analysis of APR-1400's reactor protection ssystem by using RiskSpectrum PSA. *Nucl. Eng. Des.* **2018**, *339*, 225–234. [CrossRef]
6. White, M.T.; Bianchi, G.; Chai, L.; Tassou, S.A.; Sayma, A.I. Review of supercritical CO_2 technologies and systems for power generation. *Appl. Therm. Eng.* **2020**, *185*, 116447. [CrossRef]
7. Jin, Q.; Xia, S.; Chen, L. A modified recompression S–CO_2 Brayton cycle and its thermodynamic optimization. *Energy* **2023**, *263*, 126015. [CrossRef]
8. Dostal, V.; Driscoll, M.J.; Hejzlar, P. *A Supercritical Carbon Dioxide Cycle for Next Generation Nuclear Reactors*; Massachusetts Institute of Technology: Cambridge, MA, USA, 2004.
9. Li, M.J.; Zhu, H.H.; Guo, J.Q.; Wang, K.; Tao, W.Q. The development technology and applications of supercritical CO_2 power cycle in nuclear energy, solar energy and other energy industries. *Appl. Therm. Eng.* **2017**, *126*, 255–275. [CrossRef]
10. Feher, E.G. The Supercritical thermodynamic power cycle. In Proceedings of the Intersociety Energy Conversion Engineering Conference IECEC, Miami Beach, FL, USA, 13–17 August 1967.
11. Angelino, G. Carbon dioxide condensation cycles for power production. *J. Eng. Power* **1968**, *90*, 287–295. [CrossRef]
12. Dievot, J.P. The sodium-CO_2 fast breeder reactor concept. In Proceedings of the International Conference on Sodium Technology and Large Fast Reactor Design, Argonne, IL, USA, 7–9 November 1968.
13. Gokhstein, D.P. Use of carbon dioxide as a heat carrier and working substance in atomic power station. *Sov. At. Energy* **1969**, *26*, 430–432. [CrossRef]
14. Shropshire, D.E. Lessons learned from GEN I carbon dioxide cooled reactors. In Proceedings of the Twelfth International Conference on Nuclear Engineering, Arlington, VA, USA, 25–29 April 2004.
15. National Energy Technology Laboratory. Supercritical Carbon Dioxide Technology Project Portfolin. Available online: www.ntel.doe.gov/research/coal/energysystem/SCO-technology/project-portfolin (accessed on 30 November 2016).
16. Pope, M.A. Thermal Hydraulic of a 2400 MW th Direct Supercritical CO_2-Cooled Fast Reactor. Ph.D. Thesis, Nuclear Engineering Massachusetts Institute of Technology, Cambridge, MA, USA, 2004.
17. Handwerk, C.S.; Driscoll, M.J.; Hejzlar, P. Optimized core design of a supercritical carbon dioxide-cooled fast reactor. *Nucl. Technol.* **2008**, *164*, 320–336. [CrossRef]
18. Pope, M.A.; Lee, J.I.; Hejzlar, P.; Driscoll, M.J. Thermal hydraulic challenges of Gas Cooled Fast Reactors with passive safety features. *Nucl. Eng. Des.* **2009**, *239*, 840–854. [CrossRef]
19. Wu, P.; Ma, Y.; Gao, C.; Liu, W.; Shan, J.; Huang, Y.; Wang, J.; Zhang, D.; Ran, X. A review of research and development of supercritical carbon dioxide Brayton cycle technology in nuclear engineering applications. *Nucl. Eng. Des.* **2020**, *368*, 110767. [CrossRef]
20. Dittmar, M. Nuclear energy: Status and future limitations. *Energy* **2012**, *37*, 35–40. [CrossRef]
21. Todreas, N.E.; Hejzlar, P.; Nikiforova, A.; Petroski, R.; Shwageraus, E.; Fong, C.J.; Driscoll, M.J.; Elliott, M.A.; Apostolakis, G. Flexible conversion ratio fast reactors: Overview. *Nucl. Eng. Des.* **2009**, *239*, 2582–2595. [CrossRef]
22. Rowinski, M.K.; White, T.J.; Zhao, J. Small and Medium sized Reactors (SMR): A review of technology. *Renew. Sustain. Energy Rev.* **2015**, *44*, 643–656. [CrossRef]
23. Li, Z.; Liu, X.; Shao, Y.; Zhong, W. Research and Development of Supercritical Carbon Dioxide Coal-Fired Power Systems. *J. Therm. Sci.* **2020**, *29*, 546–575. [CrossRef]
24. Available online: https://en.wikipedia.org/wiki/Carbon_dioxide (accessed on 13 September 2023).
25. Parma, E.J.; Wright, S.A.; Vernon, M.E.; Fleming, D.D.; Rochau, G.E.; Suo-Anttila, A.J.; AI, R.; Tsvetkov, P. *Supercritical CO_2 Direct Cycle Gas Fast Reactor (SC-GFR) Concept*; Sandia National Laboratories: Albuquerque, NM, USA, 2011.
26. Kimball, K.J.; Clementoni, E.M. Supercritical carbon dioxide brayton power cycle development overview. In Proceedings of the ASME Turbo Expo, Copenhagen, Denmark, 11–15 June 2012.
27. Wang, E.; Peng, N.; Zhang, M. System design and application of supercritical and transcritical CO_2 power cycles: A review. *Front. Energy Res.* **2021**, *9*, 723875. [CrossRef]
28. Fan, Y.H.; Tang, G.H.; Li, X.L.; Yang, D.L. General and unique issues at multiple scales for supercritical carbon dioxide power system: A review on recent advances. *Energy Convers. Manag.* **2022**, *268*, 115993. [CrossRef]
29. Cho, J.; Choi, M.; Baik, Y.-J.; Lee, G.; Ra, H.-S.; Kim, B.; Kim, M. Development of the turbomachinery for the supercritical carbon dioxide power cycle. *Int. J. Energy Res.* **2016**, *40*, 587–599. [CrossRef]
30. Wang, R.; Wang, X.; Shu, G.; Tian, H.; Cai, J.; Bian, X.; Qin, Z.; Shi, L. Comparison of different load-following control strategies of a sCO2 Brayton cycle under full load range. *Energy* **2022**, *246*, 123378. [CrossRef]
31. Crespia, F.; Gavagni, G.; Sanchez, D.; Martinez, G.S. Supercritical carbon dioxide cycles for power generation: A review. *Appl. Energy* **2017**, *195*, 152–183. [CrossRef]
32. Conboy, T.; Wright, S.; Pasch, J.; Fleming, D.; Rochau, G.; Fuller, R. Performance Characteristics of an operating supercritical CO_2 brayton cycle. *J. Eng. Gas Turbines Power* **2012**, *134*, 111703. [CrossRef]
33. Sienicki, J.; Moisseytsev, A.; Fuller, B.; Wright, S. Scale Dependencies of Supercritical Carbon Dioxide Brayton Cycle Technologies and the Optimal Size for a Next-Step Supercritical CO2 Cycle Demonstration. In Proceedings of the Supercritical CO2 Power Cycle Symposium, Boulder, CO, USA, 24–25 May 2011.

34. Dostal, V.; Driscoll, M.J.; Hejzlar, P.; Todreas, N.E. A supercritical CO_2 gas turbine power cycle for next-generation nuclear reactors. In Proceedings of the ICONE 10th International Conference on Nuclear Engineering, Arlington, VA, USA, 14–18 April 2002.
35. Utamura, M.; Hasuike, H.; Yamamoto, T. Demonstration test plant of closed cycle gas turbine with supercritical CO_2 as working fluid. *Strojarstvo* **2010**, *52*, 459–465.
36. Wright, S.A.; Radel, R.F.; Vernon, M.E.; Rochau, G.E.; Pickau, P.S. *Operation and Analysis of a Supercritical CO_2 Brayton Cycle*; Sandia National Laboratories: Livermore, CA, USA, 2010.
37. Uusitalo, A.; Grnman, A. Analysis of radial inflow turbine losses operating with supercritical carbon dioxide. *Energies* **2021**, *14*, 3561. [CrossRef]
38. Uusitalo, A.; Turunen-Saaresti, T.; Grnman, A. Design and loss analysis of radial turbines for supercritical CO_2 Brayton cycles. *Energy* **2021**, *230*, 12878. [CrossRef]
39. Du, Y.; Tian, G.; Pekris, M. A comprehensive review of micro-scale expanders for carbon dioxide related power and refrigeration cycles. *Appl. Therm. Eng.* **2022**, *201*, 117722. [CrossRef]
40. Engeda, A.; Chen, J. Prospect and challenges for developing and marketing a brayton-cycle based power genset gas-turbine using supercritical CO_2: Part II—The turbomachinery components design challenges. In *Turbo Expo: Power for Land, Sea, and Air*; American Society of Mechanical Engineers: New York, NY, USA, 2020; Volume 6, p. V006T08A003.
41. Cho, S.K.; Lee, J.; Lee, J.I.; Cha, J.E. S-CO_2 turbine design for decay heat removal system of sodium cooled fast reactor. In *Turbo Expo: Power for Land, Sea, and Air*; American Society of Mechanical Engineers: New York, NY, USA, 2016; Volume 9.
42. Lee, S.; Gurgenci, H. A comparison of three methodological approaches for meanline design of supercritical CO_2 radial inflow turbines. *Energy Convers. Manag.* **2020**, *206*, 112500. [CrossRef]
43. Lee, S.; Yaganegi, G.; Mee, D.J.; Guan, Z.; Gurgenci, H. Part-load performance prediction model for supercritical CO_2 radial inflow turbines. *Energy Convers. Manag.* **2021**, *235*, 113964. [CrossRef]
44. Unglaube, T.; Chiang, H.W.D. Preliminary design of small-scale supercritical CO_2 radial inflow turbines. *J. Eng. Gas. Turbines Power* **2020**, *142*, 021011. [CrossRef]
45. Senthil, K.R.; Alone, D.B.; Kumar, P. Profile loss investigations with a S-CO_2 axial turbine aerofoil. In *Turbo Expo: Power for Land, Sea, and Air*; American Society of Mechanical Engineers: New York, NY, USA, 2021; Volume 11.
46. Son, S.; Jeong, Y.; Cho, S.K.; Lee, J.I. Development of supercritical CO_2 turbomachinery off-design model using 1D mean-line method and Deep Neural Network. *Appl. Energy* **2020**, *263*, 114645. [CrossRef]
47. Dongbo, S.; Liangliang, L.; Yanyao, Z.; Xie, Y. Thermodynamic design and aerodynamic analysis of supercritical carbon dioxide turbine. In Proceedings of the 2015 International Conference on Electromechanical Control Technology and Transportation, Zhuhai City, China, 31 October–1 November 2015; Atlantis Press: Paris, France, 2015; pp. 41–44.
48. Yuqi, W.; Dongbo, S.; Di, Z.; Xie, Y. Study on aerodynamic performance of a partial-admission supercritical carbon dioxide radial-inflow turbine. *Therm. Turbine* **2016**, *45*, 184–188,195.
49. Hanzhen, Z.; Hang, Z.; Qinghu, D.; Feng, Z. Aerothermodynamic design and numerical investigation of supercritical carbon dioxide turbine. In Proceedings of the ASME Turbo Expo 2015: Turbine Technical Conference and Exposition, Montreal, QC, Canada, 15–19 June 2015.
50. Zhan, Y.; Peng, M.; Xi, G.; Wan, G.; Zhou, C. Performance analysis of S-CO_2 recompression Brayton cycle based on turbomachinery detailed design. *Nucl. Eng. Technol.* **2020**, *52*, 2107–2118. [CrossRef]
51. Wang, Y.; Liu, T.; Zhang, D. Aerodynamic prediction on the off-design performance of a S-CO_2 turbine based on deep learning. In *Turbo Expo: Power for Land, Sea, and Air*; American Society of Mechanical Engineers: New York, NY, USA, 2021; Volume 10.
52. Wang, J.; Guo, Y.; Zhou, K.; Xia, J.; Li, Y.; Zhao, P.; Dai, Y. Design and performance analysis of compressor and turbine in supercritical CO2 power cycle based on system component coupled optimization. *Energy Convers. Manag.* **2020**, *221*, 113179. [CrossRef]
53. Zhu, C.; Wen, Y.; Shao, Z. Investigation on interaction between geometry and performance and design of S-CO_2 radial inflow turbine's vaneless inlet volute. *IOP Conf. Ser. Mater. Sci. Eng.* **2020**, *1081*, 92–103.
54. Tan, W.; Wei, X.L.; Meng, X.R.; Ma, X.; Han, J. Experimental study of operating load variation for organic Rankine cycle system based on radial inflow turbine. *Appl. Therm. Eng.* **2020**, *166*, 114641.
55. Yang, J.; Zhao, F.; Zhang, M.; Liu, Y. Numerical analysis of labyrinth seal performance for the impeller backface cavity of a supercritical CO2 radial inflow turbine. *Comput. Model. Eng. Sci.* **2021**, *126*, 935–953. [CrossRef]
56. Lora-Perez, C.S.; Jauregui-Correa, J.C.A. Microturbine one-dimensional design methodology using supercritical carbon dioxide as working fluid. In Proceedings of the 14th International Engineering Congress, CONIIN, Kuala Lumpur, Malaysia, 14–19 May 2018.
57. Alshammari, F.; Karvountzis-Kontakiotis, A.; Pesiridis, A.; Giannakakis, P. Off-design performance prediction of radial turbines operating with ideal and real working fluids. *Energy Convers. Manag.* **2018**, *171*, 1430–1439. [CrossRef]
58. Du, Y.D.; Yang, C.; Hu, C.X.; Zhang, C. Thermoeconomic analysis and inter-stage pressure ratio optimization of nuclear power supercritical CO_2 multi-stage recompression. *Int. J. Energy Res.* **2020**, *45*, 2367–2382. [CrossRef]
59. Wang, X.; Liu, Q.; Lei, J.; Han, W.; Jin, H. Investigation of thermodynamic performances for two-stage recompression supercritical CO2 Brayton cycle with high temperature thermal energy storage system. *Energy Convers. Manag.* **2018**, *165*, 477–487. [CrossRef]

60. Du, Y.D.; Yang, C.; Hu, C.X.; Zhou, M. Thermodynamic design and off-design investigation of nuclear power supercritical CO_2 recompression cycle. *Nucl. Eng. Des.* **2020**, *369*, 110851. [CrossRef]
61. Park, J.H.; Cha, J.E.; Lee, S.W. Experimental investigation on performance test of 150-kW-class supercritical CO_2 centrifugal compressor. *Appl. Therm. Eng.* **2022**, *210*, 118310. [CrossRef]
62. Jeong, Y.; Son, S.; Cho, S.K.; Baik, S.; Lee, J.I. Evaluation of supercritical CO_2 compressor off-design performance prediction methods. *Energy* **2020**, *213*, 119071. [CrossRef]
63. Kim, S.G.; Cho, S.K.; Lee, J.I.; Lee, J.; Lee, S.W.; Addad, Y.; Cha, J.E. RANS simulation of a radial compressor with supercritical CO_2 fluid for external loss model development. In *Turbo Expo: Power for Land, Sea, and Air*; American Society of Mechanical Engineers: New York, NY, USA, 2018; Volume 9, p. V009T38A020.
64. Li, H.; Ju, Y.; Zhang, C. Optimization of supercritical carbon dioxide recompression Brayton cycle considering anti-condensation design of centrifugal compressor. *Energy Convers. Manag.* **2022**, *254*, 115207. [CrossRef]
65. Oh, B.S.; Jeong, Y.; Cho, S.K.; Lee, J.I. Controllability of S-CO_2 power system coupled small modular reactor with improved compressor design. *Appl. Therm. Eng.* **2021**, *192*, 116957. [CrossRef]
66. Du, Y.; Yang, C.; Wang, H.; Hu, C. One-dimensional optimisation design and off-design operation strategy of centrifugal compressor for supercritical carbon dioxide Brayton cycle. *Appl. Therm. Eng.* **2021**, *196*, 117318. [CrossRef]
67. Xia, W.; Zhang, Y.; Yu, H.; Han, Z.; Dai, Y. Aerodynamic design and multi-dimensional performance optimization of supercritical CO_2 centrifugal compressor. *Energy Convers. Manag.* **2021**, *248*, 114810. [CrossRef]
68. Pei, J.; Zhao, Y.; Zhao, M.; Liu, G.; Yang, Q.; Li, L. Effects of leading edge profiles on flow behavior and performance of supercritical CO_2 centrifugal compressor. *Int. J. Mech. Sci.* **2022**, *229*, 107520. [CrossRef]
69. Pei, J.; Zhao, Y.; Zhao, M.; Liu, G.; Yang, Q.; Li, L. Effects of inlet working condition and heat load on supercritical CO_2 compressor performance. *Nucl. Eng. Technol.* **2023**, *55*, 2812–2822. [CrossRef]
70. Aneesh, A.M.; Sharma, A.; Srivastava, A.; Chaudhury, P. Effects of wavy channel configurations on thermal-hydraulic characteristics of Printed Circuit Heat Exchanger (PCHE). *Int. J. Heat. Mass. Tran.* **2018**, *118*, 304–315. [CrossRef]
71. Li, Q.; Flamant, G.; Yuan, X.G.; Neveu, P.; Luo, L.G. Compact heat exchangers: A review and future applications for a new generation of high temperature solar receivers. *Renew. Sustain. Energy Rev.* **2011**, *15*, 4855–4875. [CrossRef]
72. Hussein, H.A.M.; Zulkifli, R.; Mahmood, W.M.F.B.W.; Ajeel, R.K. Structure parameters and designs and their impact on performance of different heat exchangers: A review. *Renew. Sustain. Energy Rev.* **2022**, *154*, 111842. [CrossRef]
73. Liu, S.; Gao, C.; Liu, M.; Chen, Y.; Tang, J.; Huang, Y.; Zhu, X.; Xing, T. An improved zigzag-type printed circuit heat exchanger for supercritical CO_2 Brayton cycles. *Ann. Nucl. Energy* **2023**, *183*, 109653. [CrossRef]
74. Nobuyoshi, T.; Yasuyoshi, K.; Konstantin, N.; Takao, I. Advanced microchannel heat exchanger with S-shaped fins. *J. Nucl. Sci. Technol.* **2009**, *46*, 403–412.
75. Lam, N.T.; Yasuyoshi, K.; Konstantin, N.; Takao, I. Heat transfer and pressure drop correlations of microchannel heat exchangers with S-shaped and zigzag fins for carbon dioxide cycles. *Exp. Therm. Fluid. Sci.* **2007**, *32*, 560–570.
76. Xiangyang, X.; Ting, M.; Lei, L.; Min, Z.; Yitung, C.; Yanping, H.; Wang, Q. Optimization of fin arrangement and channel configuration in an airfoil fin PCHE for supercritical CO_2 cycle. *Appl. Therm. Eng.* **2014**, *70*, 867–875.
77. Li, X.L.; Tang, G.H.; Fan, Y.H.; Yang, D.L. A performance recovery coefficient for thermal-hydraulic evaluation of recuperator in supercritical carbon dioxide Brayton cycle. *Energy Convers. Manag.* **2022**, *256*, 115393. [CrossRef]
78. Liu, B.; Lu, M.; Shui, B.; Sun, Y.; Wei, W. Thermal-hydraulic performance analysis of printed circuit heat exchanger precooler in the Brayton cycle for supercritical CO_2 waste heat recovery. *Appl. Energy* **2022**, *305*, 117923. [CrossRef]
79. Liu, K.; Zhao, F.; Jin, Y.; Hu, C.; Ming, Y.; Liu, Y.; Tian, R.; Liu, S. S–CO_2 heat transfer characteristics analysis in PCHE and vertical channel. *Prog. Nucl. Energy* **2022**, *154*, 104472. [CrossRef]
80. Saeed, M.; Berrouk, A.S.; Al Wahedi, Y.F.; Singh, M.P.; Dagga, I.A.; Afgan, I. Performance enhancement of a C-shaped printed circuit heat exchanger in supercritical CO_2 Brayton cycle: A machine learning-based optimization study. *Case Stud. Therm. Eng.* **2022**, *38*, 102276. [CrossRef]
81. Saeed, M.; Radaideh, M.I.; Berrouk, A.S.; Alawadhi, K. Machine learning-based efficient multi-layered precooler design approach for supercritical CO_2 cycle. *Energy Convers. Manag.* **2021**, *11*, 100104. [CrossRef]
82. Safari, Y.; Abdollahi, S.A.; Mahmoudi, M.; Safaei, M.; Taghinia, F.; Pasha, P.; Ganji, D.D. Numerical study of heat transfer of wavy channel supercritical CO_2 PCHE with various channel geometries. *Int. J. Thermofluids* **2023**, *18*, 100330. [CrossRef]
83. Robey, E.; Ramesh, S.; Sabau, A.S.; Abdoli, A.; Black, J.; Straub, D.; Yip, J. Design optimization of an additively manufactured prototype recuperator for supercritical CO2 power cycles. *Energy* **2022**, *251*, 123961. [CrossRef]
84. Lu, Y.; Guo, Z.; Gong, Y.; Zhang, T.; Huang, Y.; Niu, F. Optimal study of swordfish fin microchannel heat exchanger for the next generation nuclear power conversion system of lead-based reactor. *Ann. Nucl. Energy* **2022**, *165*, 108679. [CrossRef]
85. Riahi, S.; Belusko, M.; Lau, T.; Flewell-Smith, R.; Evans, M.; Bruno, F. Impact of different types of channels on Thermo-hydraulic performance of a sodium-sCO_2 Printed circuit heat exchanger for supercritical Brayton cycle applications. *Appl. Therm. Eng.* **2022**, *216*, 119098. [CrossRef]
86. Su, X.-K.; Li, X.-W.; Wang, X.-Y.; Chen, Q.-J.; Shi, Q.-W.; Qiu, J.; Gu, L. Numerical study on conjugate heat transfer characteristics of liquid lead-bismuth eutectic and supercritical carbon dioxide in a PCHE straight channel. *Ann. Nucl. Energy* **2023**, *186*, 109756. [CrossRef]

87. Yu, H.; Hartanto, D.; Moon, J.; Kim, Y. A conceptual study of a supercritical CO_2-cooled micro modular reactor. *Energies* **2015**, *13*, 13938–13952. [CrossRef]
88. Kim, Y.H.; Hartanto, D.; Yu, H. Neutronics optimization and characterization of a long-life SCO_2-cooled micro modular reactor. *Int. J. Energy Res.* **2016**, *41*, 976–984. [CrossRef]
89. Kim, S.G.; Yu, H.; Moon, J.; Baik, S.; Kim, Y.; Jeong, Y.H.; Lee, J.I. A concept design of supercritical CO_2-cooled SMR operating at isolated microgrid region. *Int. J. Energy Res.* **2017**, *41*, 512–525. [CrossRef]
90. Gao, C.; Wu, P.; Shan, J.; Huang, Y.; Zhang, J.; Wang, L. Preliminary study of system design and safety analysis methodology for supercritical carbon dioxide Brayton cycle direct-cooled reactor system. *Ann. Nucl. Energy* **2020**, *147*, 107734. [CrossRef]
91. Lu, D.; Ding, H.; Sui, D.; Teng, Y. Safety analysis of a supercritical carbon dioxide cooled reactor system coupled with Brayton cycle under loss-of-coolant accident. *Prog. Nucl. Energy* **2023**, *161*, 104718. [CrossRef]
92. Ding, H.; Zhang, Y.; Hong, G.; Li, J. Comparative study of the supercritical carbon-dioxide recompression Brayton cycle with different control strategies. *Prog. Nucl. Energy* **2021**, *137*, 103770. [CrossRef]
93. Xue, Q.; Wu, P.; Liu, M.; Shan, J.; Huang, Y. Thermal hydraulic design and mass optimization of a 100-kWe S-CO_2 cooled Mars-surface fission reactor system. *Ann. Nucl. Energy* **2023**, *190*, 109893. [CrossRef]
94. Fan, G.; Li, H.; Du, Y.; Chen, K.; Zheng, S.; Dai, Y. Preliminary design and part-load performance analysis of a recompression supercritical carbon dioxide cycle combined with a transcritical carbon dioxide cycle. *Energy Convers. Manag.* **2020**, *212*, 112758. [CrossRef]
95. Hofer, M.; Ren, H. Simulation and analysis of a self-propelling heat removal system using supercritical CO2 at different ambient temperatures. In Proceedings of the 4th European sCO2 Conference for Energy Systems, Online Conference, 23–24 March 2021.
96. Lim, J.; Shin, D.; Kim, T.; Park, J.H.; Lee, J.I.; Kim, S.J. Preliminary analysis of coupling supercritical CO_2 cycle and natural draft dry cooling tower for small modular reactor application. In Proceedings of the Transactions of the Korean Nuclear Society Virtual Spring Meeting, online, 13–14 May 2021.
97. Lim, J.; Jeon, J.; Park, J.H.; Shin, D.; Kim, S.J. Thermodynamic study of SCO_2 recompression brayton cycle with intercooling and reheating for light water reactor. In Proceedings of the Transactions of the Korean Nuclear Society Virtual Autumn Meeting, online, 17–18 December 2020.
98. Lee, W.W.; Bae, S.J.; Jung, Y.H.; Yoon, H.J.; Jeong, Y.H.; Lee, J.I. Improving power and desalination capabilities of a large nuclear power plant with supercritical CO_2 power technology. *Desalination* **2017**, *409*, 136–145. [CrossRef]
99. Moisseytsev, A.; Sienick, J.J. Transient accident analysis of a supercritical carbon dioxide Brayton cycle energy converter coupled to an autonomous lead-cooled fast reactor. *Nucl. Eng. Des.* **2008**, *238*, 2094–2105. [CrossRef]
100. Li, M.-J.; Jie, Y.-J.; Zhu, H.-H.; Qi, G.-J.; Li, M.-J. The thermodynamic and cost-benefit analysis of miniaturized lead-cooled fast reactor with supercritical CO_2 power cycle in the commercial market. *Prog. Nucl. Energy* **2018**, *103*, 135–150. [CrossRef]
101. Li, M.-J.; Xu, J.-L.; Cao, F.; Guo, J.-Q.; Tong, Z.-X.; Zhu, H.-H. The investigation of thermoeconomic performance and conceptual design for the miniaturized lead-cooled fast reactor composing supercritical CO_2 power cycle. *Energy* **2019**, *173*, 174–195. [CrossRef]
102. Wu, P.; Gao, C.; Huang, Y. Supercritical CO_2 brayton cycle design for small modular reactor with a thermodynamic analysis solver. *Sci. Technol. Nucl. Install.* **2020**, *2020*, 1–16. [CrossRef]
103. Li, H.; Fan, G. A comprehensive investigation on the design and off-design performance of supercritical carbon dioxide power system based on the small-scale lead-cooled fast reactor. *J. Clean. Prod.* **2020**, *256*, 120720. [CrossRef]
104. Du, Y.; Yang, C. Dynamic characteristics of a recompression supercritical CO_2 cycle against variable operating conditions and temperature fluctuations of reactor outlet coolant. *Energy* **2022**, *258*, 124774. [CrossRef]
105. Du, Y.; Yang, C. Integrated design and off-design hybrid control strategy of supercritical CO_2 recompression cycle for nuclear power. *Appl. Therm. Eng.* **2022**, *217*, 119194. [CrossRef]
106. Du, Y.; Yang, C. Research on the applicability of isothermal compressors to supercritical carbon dioxide recompression cycle for nuclear energy. *Ann. Nucl. Energy* **2023**, *180*, 109463. [CrossRef]
107. Du, Y.; Wang, L. Multi-objective optimization of thermoeconomic and component size of supercritical carbon dioxide recompression cycle based on small-scale lead-cooled fast reactor. *Int. J. Energy Res.* **2022**, *46*, 13570–13589. [CrossRef]
108. Du, Y.; Yang, C. Optimal design of a supercritical carbon dioxide recompression cycle using deep neural network and data mining techniques. *Energy* **2023**, *271*, 127038. [CrossRef]
109. Moisseytsev, A.; Sienicki, J.J. Investigation of alternative layouts for the supercritical carbon dioxide Brayton cycle for a sodium-cooled fast reactor. *Nucl. Eng. Des.* **2009**, *239*, 1362–1371. [CrossRef]
110. Eoh, J.-H.; No, H.C.; Yoo, Y.-H. Sodium-CO_2 interaction in a supercritical CO_2 power conversion system coupled with a sodium fast reactor. *Nucl. Technol.* **2011**, *173*, 99–114. [CrossRef]
111. Sienicki, J.J.; Moisseytsev, A.; Krajtl, L. Utilization of the supercritical CO2 brayton cycle wirh sodium-cooled fast reactors. In Proceedings of the 4th International Symposium–Supercritical CO2 Power Cycles, Pittsburgh, PA, USA, 9–10 September 2014.
112. Xie, M.; Cheng, J.; Ren, X. System performance analyses of supercritical CO_2 brayton cycle for sodium-cooled fast reactor. *Energies* **2022**, *15*, 3555. [CrossRef]
113. HZang, C.; Liu, X.-T.; Liu, J.; Li, Z.-E. Characteristics and optimization of SCO_2 brayton cycle system for high power sodium-cooled fast reactor on mars. *Therma Sci.* **2021**, *25*, 4659–4666.
114. Nurmayady, D. Thermal efficiency modelling for HTGR GT 10 MWth. *AIP Conf. Proc.* **2022**, *2501*, 040002.

115. Yun, S.; Zhang, D.; Li, X.; Zhou, X.; Jiang, D.; Wu, X.L.W.; Feng, Z.; Min, X.; Tian, W.; Qiu, S.; et al. Design, optimization and thermodynamic analysis of SCO_2 Brayton cycle system for FHR. *Prog. Nucl. Energy* **2023**, *157*, 104593. [CrossRef]
116. Guo, S.; Wang, B.; Tang, B.; Lin, S.; Yang, J.; Gou, L.; Dai, C.; Zhu, Y.; Wang, P.; Qian, D.; et al. Research on Megawatt-Class High-Efficiency and Compact New Marine Nuclear Power Plant. *China Basic Sci.* **2021**, *23*, 42–50. (In Chinese)
117. Mazzetti, A.; Pret, M.G.; Pinarello, G.; Celotti, L.; Piskacev, M.; Cowley, A. Heat to electricity conversion systems for moon exploration scenarios: A review of space and ground technologies. *Acta Astronaut.* **2019**, *156*, 162–186. [CrossRef]
118. Yang, J.; Yang, Z.; Duan, Y. A review on integrated design and off-design operation of solar power tower system with $SeCO_2$ Brayton cycle. *Energy* **2022**, *246*, 123348. [CrossRef]
119. Chen, J.; Liu, L.; Liao, G.; Zhang, F.; Jiaqiang, E.; Tan, S. Design and Off-design Performance Analysis of Supercritical Carbon Dioxide Brayton Cycles for Gas Turbine Waste Heat Recovery. *Appl. Therm. Eng.* **2023**, *235*, 121295. [CrossRef]
120. Wang, Z.; Jiang, Y.; Ma, Y.; Han, F.; Ji, Y.; Cai, W. A partial heating supercritical CO_2 nested transcritical CO_2 cascade powercycle for marine engine waste heat recovery: Thermodynamic, economic, and footprint analysis. *Energy* **2022**, *261*, 125269. [CrossRef]

Disclaimer/Publisher's Note: The statements, opinions and data contained in all publications are solely those of the individual author(s) and contributor(s) and not of MDPI and/or the editor(s). MDPI and/or the editor(s) disclaim responsibility for any injury to people or property resulting from any ideas, methods, instructions or products referred to in the content.